CARDIFF UNIVERSITY
PRIFYSGOL CAERDYDD

ORCA – Online Research @ Cardiff

This is an Open Access document downloaded from ORCA, Cardiff University's institutional repository:https://orca.cardiff.ac.uk/id/eprint/148082/

This is the author's version of a work that was submitted to / accepted for publication.

Citation for final published version:

Redwood, Stewart D., Buchs, David M. and Cavell, David Edward 2022. Submarine volcanic activity and giant amygdale formation along the Panama island arc as a precursor to 6000-year-old agate exploitation on Pedro González Island. Geological Magazine 159 (5) , pp. 673-688. 10.1017/S0016756821001229

Publishers page: http://dx.doi.org/10.1017/S0016756821001229

Please note:
Changes made as a result of publishing processes such as copy-editing, formatting and page numbers may not be reflected in this version. For the definitive version of this publication, please refer to the published source. You are advised to consult the publisher's version if you wish to cite this paper.

This version is being made available in accordance with publisher policies. See http://orca.cf.ac.uk/policies.html for usage policies. Copyright and moral rights for publications made available in ORCA are retained by the copyright holders.

Submarine volcanic activity and giant amygdale formation along the Panama island arc as a precursor to 6,000 year old agate exploitation on Pedro Gonzalez Island

Stewart D. Redwood [1*], David M. Buchs [2, 3], David Edward Cavell [4]

[1] Consulting Geologist, P.O. Box 0832-0757, Panama, Republic of Panama.
[2]School of Earth and Ocean Sciences, Cardiff University, Cardiff, CF10 3AT, UK.
[3]Smithsonian Tropical Research Institute, P.O. Box 0843-03092, Panama, Republic of Panama.
[4]School of Geography, Earth and Environmental Sciences, University of Birmingham, Edgbaston, Birmingham, B15 2TT, UK.
'* Corresponding author. Email address: stewart@sredwood.com

Abstract

An extensive deposit of agate occurs in Pedro Gonzalez Island in the Gulf of Panama. Previous archaeological research showed that the agate was exploited between 6,200 and 5,600 cal BP to make stone tools found at the oldest known Preceramic human settlement in the Pearl Island archipelago. We constrain here the origin and geological context of the agate through a geological and geochemical study of the island. We show that it includes primary volcanic breccias, lavas, and tuffaceous marine deposits with sedimentary conglomerates and debris flow deposits, which we define as the Pedro Gonzalez Formation. This formation records submarine to subaerial volcanic activity along an island arc during the Oligo-Miocene, confirming previous regional models that favour progressive emergence of the isthmus in the early Miocene. The igneous rocks have an extreme tholeiitic character that is interpreted to reflect magmatic cessation in eastern Panama during the early Miocene. The agate is hosted in andesitic lavas in unusually large amygdales of up to 20-40 cm in diameter, as well as small amygdales (0.1-1.0 cm) in a bimodal distribution, and in veins. The large size of the agates made them suitable for tool manufacture. Field evidence suggests that the formation of large amygdales resulted from subaqueous lava-sediment interaction, in which water released from unconsolidated tuffaceous deposits at the base of lava flows rose through the lavas, coalesced, and accumulated below the chilled lava top, with subsequent hydrothermal mineralisation. These amygdales could therefore be regarded as an unusual result of combined peperitic and hydrothermal processes.

Keywords: Gulf of Panama; volcanic islands; vesicles; peperitic processes; Preceramic archaeological site

1. Introduction

An extensive deposit of agate occurs on Pedro Gonzalez Island in the Pearl Island archipelago of the Gulf of Panama (Figs. 1-2). Archaeological studies showed that the agate was exploited to make abundant stone tools between 6,200 and 5,600 cal BP, which were found at an accumulation of cultural debris at Don Bernardo Beach on the north-eastern coast of Pedro González Island (Fig. 3). This represents the oldest Preceramic human settlement yet identified in the Pearl Island archipelago, where there is clear evidence for exploitation of dolphins and other marine and terrestrial fauna using the agate tools (Martin *et al.* 2016;

Cooke *et al*. 2016; Pearson *et al.* 2021). Several environmental and societal reasons could account for the existence of this settlement, but it is likely that local agate resources contributed to developing and sustaining local human activities. Some preliminary observations suggest that the agate occurs in giant amygdales in "basalt" lavas (Cooke *et al.* 2016), but the geological context and origin of the agate remain to be investigated in detail. Giant amygdales are very rare in the geological record and are generally associated with subaerial lavas (*e.g.* Shipboard Scientific Party, 2000; Self *et al.* 1997, 1998; Thordarson, 2000; Barreto *et al.* 2017), making their occurrence on Pedro Gonzalez Island a valuable opportunity to better understand their possible modes of formation. In addition, little geological information exists in eastern Panama due to logistical limitations and tropical vegetation in the most remote parts of the country. This means that new data from Pedro Gonzalez Island can help fill a large observation gap, providing novel constraints on the geological evolution of the eastern part of the Panama volcanic arc that is considered by many authors to be associated with the emergence of the Isthmus of Panama (*e.g.* Coates *et al*. 2004; Farris *et al.* 2011; Montes *et al.* 2015; Buchs *et al.* 2019a).

This study provides the first detailed lithological descriptions and geochemical analyses of Oligo-Miocene volcano-sedimentary sequences in the Pearl Island archipelago, and presents new constraints on the nature and origin of unusually large (up to 40 cm in diameter) amygdales and less abundant geodes (hereafter collectively called amygdales) that locally occur in submarine lavas. Our results suggest that the formation of the giant amygdales resulted from sediment-lava (peperitic) interaction and subsequent hydrothermal activity. As discussed below, only two other possibly similar occurrences could be found in previous studies worldwide. In addition, geochemical results show the occurrence of unusually tholeiitic supra-subduction igneous rocks, which we propose to be a lateral analogue of early Miocene volcanic deposits of the Panama Canal area and provides the first possible record of magmatic cessation in eastern Panama. New constraints on the origin of the volcano-sedimentary deposits of Pedro Gonzalez Island are consistent with previous regional studies that suggest that the Panama volcanic arc was an island arc, and not yet fully emergent in the early Miocene.

2. Geological Setting

The Pearl Island archipelago and Pedro Gonzalez Island are part of the East Panama Deformed Belt in the forearc of the Panama volcanic arc (Fig. 1), where a complex system of NW-SE trending, locally active, faults and trusts define several basement highs and basins filled by Eocene to Holocene sedimentary deposits (Mann & Kolarsky, 1995; Derksen *et al.* 2003). The Pearl Islands correspond to a N-S trending basement high, which is interpreted, based on 2D seismic profiles in the Gulf of Panama, as a hanging-wall anticline associated with an east-dipping reverse fault zone (Mann & Kolarsky, 1995). This basement high separates tilted basins in the east and west of the gulf, which are locally filled by km-thick sedimentary sequences. From a regional volcanic perspective, the studied area occurs in the forearc of the latest Cretaceous to Eocene (ca. 66 to 39 Ma) Chagres-Bayano Arc that extends along the San Blas Cordillera (Wegner *et al.* 2011; Montes *et al.* 2012a) (Fig. 1). In contrast to western Panama where post-Eocene (still on-going) volcanic activity has formed a high Central Cordillera (Wegner *et al.* 2011), only limited post-Eocene volcanic activity has been documented in eastern Panama. Supra-subduction magmatism occurred in the Majé Range and Canal area during the Oligocene to early Miocene (Farris *et al.* 2011, 2017; Rooney *et al.*

2011; Whattam *et al.* 2012; Buchs *et al.* 2019a, 2019b). However, younger volcanism has not been documented yet in eastern Panama. Magmatic cessation occurred ca. 16 Ma ago in the Canal area, which could also correspond to the end of volcanism in eastern Panama (Buchs *et al.* 2019b). As further discussed below, only 2 samples of igneous rocks have been analysed and dated in the Pearl Island archipelago (Lissinna, 2005), which suggest the occurrence of early Miocene (ca. 22 to 18 Ma) arc volcanism in the studied area. However, the exact nature and extent of this volcanism, as well as its relationship with regional magmatic activity, remain very poorly constrained.

Although the regional tectono-stratigraphic context of the Pearl Island archipelago seems reasonably well constrained, very limited information exists on the geology and palaeo-environmental evolution of the Pearl Islands. To date, the only published stratigraphic study of the archipelago is from Mann & Kolarsky (1995); it provides a geological synthesis and interpretation based on data from (1) unpublished reports from the Dirección General de Hidrocarburos of Panama, (2) 1,600 km of 2D seismic surveys by Mobil Exploration and Production Services Company collected between 1969 and 1972, and (3) two offshore well logs of the El Paso Corvus-1 (2,926 m deep) and El Paso Plaris-1 (2,867 m deep) wells drilled by El Paso Natural Gas in 1974 (Fig. 2; Quirós Ponce, 1975). According to Mann & Kolarsky (1995), microfossils from marine sedimentary sequences along the eastern coast of Isla del Rey (the largest island in the archipelago) indicate a late Miocene-Pliocene age and a middle neritic or deeper environment of deposition. In sedimentary sequences of the southern part of Isla del Rey, larger benthic foraminifera indicate an Oligocene age and a very shallow inner neritic environment of deposition. These sequences are thought to correlate to basin fill sediments drilled at El Paso Corvus-1 and El Paso Plaris-1 holes located to the southwest and southeast in the Gulf of Panama (Mann & Kolarsky, 1995) (Fig. 1). In addition, correlation between these 2 drilling sites and interpretation of seismic profiles in the Gulf of Panama suggests that the geology of the area is composed of a Cretaceous to Paleogene (?) igneous basement overlain by middle Eocene conglomerate (of unspecified lithological composition) (Mann & Kolarsky, 1995). The basement sequence is, in turn, overlain above an angular unconformity by a sequence of Oligocene to Miocene marine sedimentary deposits. Overlying Plio-Pleistocene marine sediments are separated from the Oligo-Miocene sequences by another angular unconformity. The geological compilation map of the Pearl Islands presented in Mann & Kolarsky (1995) and reproduced in Fig. 2 follows this general stratigraphic subdivision, with local occurrences of small Cenozoic igneous intrusions (Fig. 3). Geochemical and geochronological data of a basaltic andesite and dacite from Isla del Rey and Bajo Bayonera islands indicate supra-subduction geochemical affinities with 21.9 ± 0.7 Ma and 18.4 ± 0.3 Ma (early Miocene) crystallization ages determined by Ar-Ar dating (Lissinna, 2005). However, the field context is not specified for these samples, and our personal geological observations at the reported sampling sites did not allow us to identify the provenance of these samples.

The stratigraphy of the Pearl Island archipelago summarised above and in Fig. 2 is in broad agreement with other field and biostratigraphic constraints from sedimentary sequences exposed further east in Panama (Coates *et al.* 2004; Barat *et al.* 2014). Notably, it was suggested that the former stratigraphy of the Pearl Islands (Mann & Kolarsky, 1995) can be correlated with the San Blas Complex, Darien and Clarita Formations of the Chucunaque-Tuira Basin in the Darien Province of eastern Panama (Coates *et al.* 2004; Barat *et al.* 2014).

However, it is important to note that there remain considerable gaps in our understanding of the geology and volcanic history of the Pearl Islands and eastern Panama. Although Pedro Gonzalez island has been interpreted to include an Eocene basal conglomerate (Mann & Kolarsky, 1995), to our knowledge no direct constraints exist on the geology of the island. In addition, early Miocene ages of crystallization of the 2 igneous samples with arc geochemical affinities by Lissinna (2005) are not consistent with the interpretation of a Cretaceous to Paleogene (?) igneous basement in the area (Mann & Kolarsky, 1995). However, the geochemistry of these samples has not yet been compared with that of the Cretaceous to recent volcanic fronts of Panama, and no geochemical data exists for Pedro Gonzalez Island. In fact, it remains unclear based on published geological information whether the archipelago is exclusively composed of volcanic arc products or also includes accreted oceanic islands and autochthonous oceanic plateau sequences similar to those exposed elsewhere in the Panamanian forearc (*e.g.* Buchs *et al.* 2011). This study helps address some of these issues with new detailed field observations and a comparison of new geochemical data from igneous rocks of Pedro Gonzalez Island with other well-dated volcanic units of Panama.

3. Methods

3.a. Field observations and sampling

Mapping of Pedro Gonzalez Island was carried out iteratively during 3 field campaigns between 2009 and 2016. Because the island has a low topography and is covered by tropical forest, lithological observations and sampling were focused on coastal exposures at low tide from a boat or along beaches, where possible. A full coverage of coastal exposures was achieved.

3.b. Geochemical analyses and compilation of regional geochemical data

Whole rock samples weighing about 250-500 g were prepared and analysed at the School of Earth and Ocean Sciences at Cardiff University. The weathered edges were first removed by hammering and sawing. Samples were then crushed using a steel jaw crusher. An aliquot of approximately 80 ml of the crushed fraction was subsequently milled to <125 µm in an agate planetary ball mill. Approximately 2-3 g of this sample powder was heated to 900°C for two hours in a furnace to remove any volatile substances and determine loss on ignition (LOI) values. Samples were prepared for ICP analysis using the lithium metaborate fusion method. 0.1 ± 0.001 g of each ignited sample was mixed with 0.6 ± 0.001 g of flux (50:50 lithium borate: sodium borate) in a platinum crucible and 3–4 drops of lithium iodide wetting agent were added. The mixture was fused using a Claisse Fluxy automated fusion machine. The resulting borate glass was then dissolved in a 50 ml solution of 20 ml of 10% HNO_3 and 30 ml of 18.2 Ω deionised water obtained using a Milli-Q purification system. After the mixture had fully dissolved, 1 ml of 100 ppm Rb spike was added to the solution which was then made up to 100 ml with 18.2 Ω deionized water. Approximately 20 ml of each solution was run on a Jobin Yvon Horiba Ultima 2 inductively coupled mass optical emission spectrometer (ICP-OES) to obtain major element and some trace element abundances. An aliquot of 1 ml of each solution was added to 1 ml of In and Tl and 8 ml of 2% HNO_3 and run on a Thermo Elemental X7 series inductively coupled plasma mass spectrometer (ICPMS) to obtain trace element abundances. The accuracy of the data was assessed using International Standard Reference Materials (ISRM) JB1a, JG1a and JA2 analysed alongside the samples. Major and trace element analyses of these reference materials fell within 5-10% of reference values for the majority of elements analysed, with r^2 values of >0.995 for all elements in both ICP-OES and ICP-MS

analyses. Complete analyses, including values for the ISRM, are provided in the Supplementary Data (Table S1).

Regional datasets used for comparison with new geochemical results include igneous samples from: (1) the pre-Oligocene Chagres-Bayano Arc (n=95, Wegner *et al.* 2011); (2) the post-Eocene Cordilleran Arc (n=116, Wegner *et al.* 2011), grouped here with the Early Miocene Majé Range (n=17, Whattam *et al.* 2012) and the Oligocene Cerro Patacon and Bas Obispo Formations in the Canal area (n=22, Rooney *et al.* 2011; Farris *et al.* 2017; Buchs *et al*. 2019a, 2019b); (3) early Miocene Las Cascadas and Pedro Miguel Formations from the Canal area (n=68, Farris *et al.* 2017; Buchs *et al.* 2019a, 2019b); and (4) Isla del Rey and Bajo Bayonera islands in the Pearl Islands (n=2, Lissinna, 2005). We did not include samples from Baker *et al.* (2015) from Cobre Panama, which are affected by alteration in a highly mineralised area. Samples with unrealistic Nb/Ta values of >28 (Wegner *et al.* 2011) were not plotted in trace element diagrams using Nb. Unless specified otherwise, we did not plot samples with LOI > 4 wt% in diagrams using elements that are mobile during low-temperature alteration and weathering (*e.g.* TAS and AFM diagrams). All major element contents were recalculated on an anhydrous basis before plotting. A high content of calcite in our sample DB16-104 is indicated by CaO = 16.20 wt% and LOI = 8.34 wt%. This sample was therefore not used in major element diagrams.

4. Results

4.a. Geological map and lithostratigraphy

The geology of the studied island can be subdivided into 3 main lithostratigraphic units: (1) lavas; (2) volcanic breccias; and (3) tuffaceous marine deposits (Figs. 4-6). The bedding of layered units does not follow a preferential orientation, but the dip is generally <20°. Faults are common along coastal exposures. Their significance is difficult to assess due to limited exposures and a lack of good stratigraphic markers at the scale of the island, but their frequency clearly impedes construction of a detailed/measured lithostratigraphic column in the study area. In addition, a main N-S trending fault crosscuts the island, which we introduce here as the “Pedro Gonzalez Fault”. This fault is associated with a lower topography and marks the contact between contrasted lithological assemblages in the western and eastern sides of the island. The strike of the fault is parallel to the orientation of many coastal segments around the island (Figs. 3-4). This and the location of the island suggests that the Pedro Gonzalez Fault could belong to the N-S trending reverse fault system believed to be associated with the Pearl Islands anticline (Mann & Kolarsky, 1995). However, this hypothesis could not be verified because the fault plane is preferentially weathered and was not found in field exposures.

The western side of the island is predominantly composed of volcanic breccias (Fig. 4). As shown by geochemical results presented below, these breccias and other igneous rocks of Pedro Gonzalez Island have basaltic andesite to andesite compositions; these will be informally referred to as “andesitic” thereafter. The breccias are monomictic and grain supported, with poorly sorted and generally angular to amoeboid clasts (Figs. 5E-G). Some of the clasts have a chilled/quenched glassy margin that can be locally palagonized (Figs. 5F-G). The breccias are commonly crosscut by andesitic dykes that form <5% of the unit. The igneous rocks of this unit are generally devoid of vesicles and amygdales. Although no pillow lavas were observed, the lithostratigraphic, compositional and textural characteristics of the

breccias indicate that they represent primary volcanic products emplaced in a subaqueous environment.

The eastern side of the island that hosts the Don Bernardo archaeological site includes a distinct sequence composed of andesitic lavas interbedded with tuffaceous marine deposits and minor volcanic breccias (Fig. 4). Andesite dykes and small igneous intrusions form a very minor fraction (<5%). A topographic high in the interior of the island could be the erosional remnant of a larger intermediate/felsic intrusion (Fig. 3). The lavas vary greatly in thickness and morphology, from relatively thin (<2m thick) lobate (Fig. 5B) to thick (~8m thick) massive or columnar-jointed lavas (Figs. 5C-D). However, no pillow lavas were observed. Auto-brecciation of some of the lavas locally occurs, apparently leading to the formation of monomictic volcanic breccias similar to those observed in the western side of the island (Figs. 5A, H). Load structures and/or brecciation of the lavas are commonly observed at the contact with tuffaceous deposits (Figs. 5A, C). Lavas also locally protrude into underlying tuffaceous deposits (Fig. 5B). These lithofacies provide clear evidence for interaction of submarine lava flows with soft (water-rich) marine sediments, which locally led to peperitic brecciation (*e.g.* Skilling *et al.* 2002).

Tuffaceous marine deposits form approximately 50% of the lithologies mapped on the eastern side of the island (Fig. 4). These deposits have a distinctive light brown colour with a rare calcareous component. Alteration of finer volcanic (tuffaceous) components is extensive in this lithology. The sequences are generally sandy and well-bedded, with frequent cross-laminae and cross-bedding, and occasional *Thalassinoides*(?) burrows (Fig. 6). The tuffaceous component of this lithology is best illustrated in the field by occasional pumice-rich layers, which can form discrete 1 to 30-cm thick intervals/lenses in the otherwise generally finer deposits (Fig. 6C). These lithofacies are interpreted as (1) relatively pure, undisturbed volcanic fallout tuffs, and (2) a mixture of fallout tuffs with minor pelagic sediments, which were partly to totally homogenized by burrowing and reworking by bottom currents. In addition, some of the thicker beds of the tuffaceous marine deposits can from tabular beds and lenticular bodies (*e.g.* Fig. 6A), which commonly lack internal structure and include a large abundance of granules to boulders of petrographically diverse andesite (Figs. 6A, B, D). The igneous clasts are poorly sorted and very angular to well rounded. These clast-rich matrix- to grain-supported tuffaceous lithologies are interpreted to have formed from debris flows and grain flows with local slumps. Turbidites do not occur in the sequence. Fast sedimentation rates of the tuffaceous deposits can be inferred based on the common occurrence of fluid escape structures (Fig. 6D), and the lack of intervals of finer-grained fossiliferous (calcareous, clayey, or siliceous) lithologies from a background pelagic sedimentation.

4.b. Whole-rock petrography and geochemistry

Nine samples of igneous rocks were selected for whole-rock analysis, including 3 lavas with minor to no vesicles, 1 lava host to giant amygdales, 2 dykes cross-cutting tuffaceous deposits and primary volcanic breccias, and 3 clasts from primary volcaniclastic deposits (Supplementary Table S1; the sample locations are shown in Fig. 4). Field constraints indicate that all samples are representative of local magmatic activity. Microscope observations show that the samples are poorly porphyritic, with feldspar and/or clinopyroxene phenocrysts and display amygdales only in a few rare occurrences (Fig. 7). A variable, albeit generally minor, degree of alteration is shown by LOI that ranges between 1.3 and 8.3 wt%. Thin sections show

that glass and plagioclase microlites are commonly replaced by clays and opaque minerals (presumably Fe oxides and hydroxides). Larger plagioclase phenocrysts commonly have a sieve texture that attests to magma mixing and/or disaggregation of crystal mush in the magma plumbing system. However, despite evidence for minor alteration and magma mixing and/or mineral accumulation, the composition of the samples is overall very consistent and supports the occurrence of a single, cogenetic magmatic suite on Pedro Gonzalez Island (Figs. 8-9).

The studied igneous rocks are basaltic andesite to andesite (Fig. 8A) that plot in the tholeiitic field of the AFM diagram (Fig. 8B). This clearly contrasts with the bulk of the Panama volcanic arc that has calc-alkaline affinities. The sample hosting giant amygdales is an andesite (SiO_2 = 60.6 wt%, LOI = 3.6 wt%) without any distinctive geochemical features. Consistent with their AFM tholeiitic affinities, the Pedro Gonzalez igneous rocks have particularly high FeO*/MgO and CaO/Al_2O_3 values at a given SiO_2 content (Figs. 8C, D). These features are commonly associated with delayed Fe-oxides and earlier feldspar crystallization in anhydrous melts (*e.g.* Arculus, 2003; Schmidt & Jagoutz, 2017), hence supporting lower water contents in the magmas of Pedro Gonzalez relative to the bulk of the Panama volcanic arc. When compared to other igneous rocks of the Panama volcanic arc, the Pedro Gonzalez samples are more akin (but not identical) to tholeiitic basalts to dacites of the Panama Canal area (early Miocene Las Cascadas and Pedro Miguel Formations, *e.g.* Buchs *et al.* 2019b) (Fig. 8). Normalised patterns of immobile trace elements are very consistent within Pedro Gonzalez samples and document supra-subduction magmatic affinities with a gradual increase in the most incompatible elements punctuated by a typical Nb-Ta negative anomaly (Fig. 9A). These trace element patterns are broadly similar to the average composition of the post-Eocene Panama volcanic arc (see Methods for the full list of references) and a sample of early Miocene dacite from Isla del Rey in the Pearl Island archipelago (Lissinna, 2005). Geochemical similarity to the post-Eocene Panama volcanic arc is also supported by Nb/Yb vs Th/Yb and La/Sm vs Nb/Th diagrams (Figs. 9B, C). In addition, these diagrams show that Pedro Gonzalez samples are compositionally distinct from the Isla del Rey dacite of Lissinna (2005). Importantly, MgO vs TiO_2 trends show that about half of the analysed Pedro Gonzalez igneous rocks have a much higher TiO_2 content at a given MgO than the bulk of the post-Eocene volcanic arc, including early Miocene samples from the Pearl Island archipelago (Lissinna, 2005) and Majé Range (Whattam *et al.* 2012) (Fig. 9D). High TiO_2 contents have only been previously observed in tholeiitic series of the Panama Canal area (ca. 21 to 16 Ma) that are associated with magmatic cessation in central Panama (Buchs *et al.* 2019b).

4.c. Agate deposit

Agate occurs in unusually large amygdales, and fewer geodes, of up to 20-40 cm in diameter, as well as small amygdales (0.1-1.0 cm) in a bimodal distribution, and in veins in vesicular andesitic lavas over a zone of about 2.9 km N-S by up to 1.3 km wide, with an area of about 3.0 km^2, on the Punta Zancadilla peninsula and around Don Bernardo and Mague beaches on the north-eastern part of Pedro Gonzalez Island (Figs. 3-4, 10). The amygdales only occur in a few andesitic lavas interbedded with tuffaceous sediments, which clearly indicate that unusual, favourable lithostratigraphic conditions were required for their formation. Some of the large amygdales are found in laterally continuous, planar lavas which often have columnar jointing, with more abundant and larger amygdales in the upper parts (Figs. 10A, B, F). The

other large amygdales occur in the front of shorter, lobate lavas which form arcuate or ring structures several metres across (Figs. 10C-E).

Agate (and rarely quartz) occurs in the amygdales and in irregular veins and vein breccias up to 20 cm wide that cross-cut both the lavas and amygdales (Figs.10E-F; Fig. 11). The small amygdales may have a wall contact layer of an acicular brown mineral, possibly a zeolite, infilled with agate, quartz and late calcite (Figs 11A,B,D), and some small amygdales have a thin wall-contact layer of agate or quartz that is coated by an unidentified botryoidal mineral and infilled by coarse calcite (Fig. 11C). The vein structures have an associated narrow halo of weak intermediate argillic alteration and bleaching to clays, probably smectite, which makes the basalt softer and more readily eroded. Agate veins were seen in tuffaceous sediments adjacent to one flow, but are generally absent in sedimentary rocks that are interbedded with the lavas. The colour of the agate is medium grey to white, and some have weak concentric colour banding and textural banding, particularly in veins. A thin section cut across a large agate amygdale shows it to be zoned from chalcedony with a fibrous radial texture in spherules on the edge (Fig. 11E), to microgranular chalcedony laths <50 um long in the middle (Fig. 11F). Open centres occur in some amygdales, which are thus termed geodes, and some veins, and may be lined with very small to rarely coarse quartz crystals. The hard agate nodules are resistant to weathering and are abundant in the soils over the lavas, and in gravel beaches, although in the latter they are often broken and the agate whitened by reaction with seawater. However, the agate in these deposits is very hard and could be easily extracted and processed to create sharp tools.

The size of the agate-filled amygdales, commonly up to 20 cm in diameter and occasionally up to 40 cm, is highly unusual. The height is much less than the diameter. Small amygdales (0.1-1.0 cm) occur together with large ones to give a bimodal size distribution. The amygdales have a flat base with a domed top, although some can be very flat, are circular to less commonly oval in plan, and are usually aligned in the basalt in flow textures (Fig. 10). There is clear evidence for bubble coalescence at all observed localities (Fig. 10C).

5. Discussion

5.a. Geology of Pedro Gonzalez Island and palaeogeographic implications

The geology of Pedro Gonzalez Island was previously considered to be a basal conglomerate of mid Eocene age (Mann & Kolarsky, 1995; Fig. 2). Middle Eocene conglomerates and shallow-marine limestones rich in larger benthic foraminifera are commonly exposed in the Panamanian forearc, where they usually underlie km-thick turbiditic to hemipelagic volcaniclastic/tuffaceous sedimentary sequences (*e.g.* Kolarsky *et al.* 1995; Krawinkel *et al.* 1999; Buchs *et al.* 2011; Montes *et al.* 2012b; Barat *et al.* 2014). These basal conglomerates and shallow marine limestones likely mark a tectonically-induced regional subsidence of the outer margin (Buchs *et al.* 2011). In contrast, geological observations at Pedro Gonzalez Island indicate the occurrence of a complex assemblage of primary volcanic andesitic breccias, andesitic lavas, tuffaceous marine deposits, and minor andesitic dykes. This lithological assemblage clearly supports a deeper marine environment with active volcanic activity, unlike shallow marine environments recorded by regional middle Eocene conglomerates exposed elsewhere in the Panamanian forearc. In addition, our regional
geologic reconnaissance in the Pearl Islands suggests that Pedro Gonzalez lithostratigraphy is similar to that of sedimentary sequences and igneous rocks dated between the Oligocene and

early Miocene on Isla del Rey (Mann & Kolarsky, 1995; Lissinna, 2005). In contrast to the information on the existing geological map (Fig. 2), we have not yet found exposures of pre-Oligocene igneous basement overlain by shallow-marine limestones and conglomerates in the Pearl Islands. In addition, new geochemical results indicate that igneous rocks on Pedro Gonzalez Island are compositionally similar to the post-Eocene volcanic arc, and most particularly to the early Miocene tholeiitic sequences of the Canal area that are associated with magmatic cessation in central Panama ca. 16 Ma ago (Buchs *et al.* 2019b) (Figs. 8-9). As indicated by the AFM diagram and FeO*/MgO and CaO/Al_2O_3 ratios (Fig. 8), the analysed igneous rocks have the most extreme tholeiitic character found to date in Panama. This is consistent with the hypothesis that a decrease of hydrous slab component accompanied magmatic cessation regionally (Farris *et al.* 2011; Buchs *et al.* 2019b). Therefore, the unusual composition of Pedro Gonzalez igneous suite suggests emplacement during or shortly before magmatic cessation, which is constrained to ca. 16 Ma based on previous data from the Canal area (Buchs *et al.* 2019b). This age of emplacement is also broadly consistent with previous geochronological constraints from igneous rocks in the Pearl Island archipelago (Lissinna, 2005), although caution is required in this comparison considering observed geochemical differences with Pedro Gonzalez Island (Fig. 9) These age constraints are additionally in agreement with biostratigraphic data from the El Paso Plaris-1 drill hole (Fig. 1), which we consulted at the National Secretariat of Energy of Panama in 2016, and indicates the occurrence of early Miocene planktonic foraminifera in the lowermost part of the hole at a depth of 2,776 m (i.e., *Globigerina dissimilis* and *Globigerina binaiensis*). We conclude therefore, based on these observations, that the volcano-sedimentary deposits on Pedro Gonzalez Island must represent a new formation of Oligo-Miocene age (between 34 and 16 Ma), most probably ca. 21-16 Ma based on regional geochemical and geochronological constraints and the model of magmatic cessation in central Panama (Buchs *et al.* 2019b). The newly-defined Pedro Gonzalez Formation is expected to be stratigraphically above Eocene units imaged in seismic profiles in the Gulf of Panama (Mann & Kolarsky, 1995; Derksen *et al.* 2003; Barat *et al.* 2014). It could be mapped and recognised in seismic profiles regionally, with a lithostratigraphic subdivision similar to that shown on our geological map (Fig. 4).

The volcano-sedimentary sequences of Pedro Gonzalez Island provide a novel insight into palaeo-environments in south-eastern Panama during the Oligo-Miocene. Recent stratigraphic studies from the Panama Canal area, approximately 100 km to the NW of the Pearl Islands (Fig. 1), document at least two marine transgression events between the Oligocene and early Miocene, which are correlated with: 1) neritic to bathyal sedimentation in the Eocene to Oligocene Gatuncillo, Caimito, Bohio and Bas Obiso Formations, and 2) the early Miocene Culebra Formation (Kirby *et al.* 2008; Montes *et al.* 2012b; Buchs *et al.* 2019a). During this time interval, the canal area was a terrestrial to subaqueous coastal environment host to several volcanic centres and a monogenetic volcanic field (Retallack & Kirby, 2007; MacFadden *et al*. 2014; Farris *et al.* 2017; Buchs *et al.* 2019a). In contrast, the study of forearc basins in eastern Panama indicates that Oligo-Miocene sedimentation occurred in neritic to bathyal environments, with so far, no evidence for subaerial sedimentation or extensive volcanism (Coates *et al.* 2004; Barat *et al.* 2014). Magmatic activity in the eastern Panamanian forearc during the early Miocene is, however, suggested by local reports of andesitic volcanism with ca. 20 Ma U-Pb ages in the Majé Range (Whattam *et al.* 2012), and a 21.7 ± 0.3 Ma Ar-Ar age in the Sapo Range (Lissinna, 2005), respectively 50 km to the NE and SE of the Pearl Islands (Fig. 1). The occurrence of lavas, dykes and primary volcanic breccias at Pedro

Gonzalez Island (this study) and 2 samples of igneous rocks from Isla del Rey and Bajo Bayonera (Lissinna, 2005) suggest that volcanic activity also occurred in the Pearl Islands area during the Oligo-Miocene. In addition, the observations of abundant tuffaceous deposits with cm-sized pumices and well-rounded boulders of basalt/andesite in the volcano-sedimentary deposits is clear evidence for the occurrence of active volcanic islands in or close to the Pearl Islands in this period. Thus, the studied sequences most likely formed on the slopes of an active island arc volcano. Although the depth of deposition is not precisely known, the absence of hummocky and swaley cross-stratification suggests an environment below the wave base (*i.e.* below approximately 150 m). Importantly, new observations from Pedro Gonzalez Island suggest the existence of an uncharted Oligo-Miocene volcanic front with ancient islands in the Gulf of Panama, which might have extended across the eastern Panamanian forearc from the Canal area to the Sapo Range, but of which the exact spatial extent and duration of magmatic activity remain to be investigated.

5.b. Origin of large agate-filled amygdales

5.b.1. Formation of giant vesicles

The large size of the Pedro Gonzalez agate amygdales is highly unusual and was important in making them suitable for tool manufacture at the Don Bernardo archaeological site (Cooke *et al.* 2016; Martin *et al.* 2016; Pearson *et al.* 2021). Although very limited information exists on vesicle formation in submarine lavas, the most common explanation for the formation of giant vesicles in subaerial basic lava flows is coalescence of rising gas bubbles, which can lead to the accumulation of larger, dome-shaped vesicles at the top of the lava (*e.g.* Self *et al.* 1997, 1998, Thordarson, 2000; Barreto *et al.* 2017). These characteristics are very similar to those of giant amygdales observed in Pedro Gonzalez submarine lavas (Fig. 10), which suggest that coalescence of rising vesicles played a key role in their formation. In addition, it is well documented that lava inflation and magma degassing during crystallization can control the size and distribution of vesicles in subaerial lavas (*e.g.* Self *et al.* 1996; Cashman & Kauahikaua, 1997). Although inflation could have occurred to create the morphology of some of the thicker lavas at Pedro Gonzalez Island, giant amygdales were also found in thinner lobate lavas, therefore suggesting that lava inflation was not a primary cause for the coalescence of giant vesicles in the study area. In addition, most of the lavas and igneous clasts in the study area do not contain vesicles, although our geochemical results indicate that they belong to a cogenetic magmatic suite. This suggests that the source of the volatiles to form giant amygdales was spatially restricted and non-magmatic. A simple hypothesis to account for these observations is that bubble-forming water/steam was provided from the tuffaceous sediments that underlie the lavas with giant amygdales. The release of water/steam from water-rich sediments at the contact with lavas or igneous intrusions is a common process in shallow subaqueous environments and subvolcanic settings where magma interacts with unconsolidated (water-rich) sediments/tuffs such as those observed on Pedro Gonzalez Island (*e.g.* Skilling *et al.* 2002). A magma-sediment interaction leading to the formation of giant amygdales is also in agreement with dewatering structures observed in some tuffaceous sediments interbedded with the lavas (Fig. 6D), and the peperitic textures seen the base of some lavas overlying the sediments (Fig. 5C). Efficient transfer of sediment fluids into the lava could also explain why giant vesicles could form in relatively deep marine conditions (most likely below the wave base), considering that hydrostatic pressure generally tends to suppress vesiculation in the deep sea. In this scenario, vesiculation could also have been facilitated by the formation of a non-porous rigid (quenched) crust on top of the submarine flows, which

could have facilitated fluid saturation in the crystalizing magma in the interior of the lava flow. In addition, volatile escape might also have been limited by high viscosity of the andesitic lavas. In any case, the local occurrence of large lenticular amygdales parallel to the flow direction (Fig. 10D) indicates that giant vesicles formed before the lava interior had stopped flowing. In contrast to the formation of agates in basic volcanic rocks in vesicular cavities, the formation of giant agates in acidic volcanic rocks occurs in cavities of spheroidal crystallisation or megaspherulites (high-temperature crystallisation domains) in which so called lithophysae (thundereggs) form in sizes of several cm to dm, and in extreme cases >4 m in diameter (Götze *et al.* 2020; Breitkreuz *et al*., 2021). The limited degree of alteration of the studied igneous rocks (Table S1 and Fig. 7) as well as the coalescent shape of some of the giant amygdales (Fig. 10c) are strong evidence that the amygdales cannot simply result from post-volcanic hydrothermal opening and filling of cavities as notably suggested for some subaerial lavas of the Parana large igneous province (e.g., Hartmann & Duarte, 2020).

Although the formation of giant vesicles in submarine lavas is expected to be rare, another example of sediment-lava interaction associated with large vesicles is reported from ODP Site 1139 on the Kerguelen Plateau, in a sequence of lavas emplaced in a shallow-marine (neritic) environment (Shipboard Scientific Party, 2000). At this locality, a massive lava with vesicles up to 6 cm in size intrudes a clayey sediment, with a texture typical of lobate peperites. Although the origin of these vesicles remains unclear (Shipboard Scientific Party, 2000), it is interesting to note that other lavas at Site 1139 do not have large vesicles, therefore suggesting that sediment dewatering was essential in the formation of larger vesicles.

To our knowledge, the wet sediment-lava interaction for the formation of amygdales was first proposed by Butler & Burbank (1929) for the subaerial flood basalts of the Meso-Proterozoic (1185-1085 Ma) Keweenaw Series of the Midcontinental Rift System of the USA, a large igneous province exposed in the Lake Superior region, where the amygdales contain important deposits of native copper and, accordingly, are well studied (Nicholson *et al*., 1992; Ernst & Jowitt, 1993). There it was observed that the basal amygdaloidal zones in basaltic lava flows are “more strongly developed above sedimentary beds than above other flows [which] suggests that the gas that filled the cavities may have been in part derived from the underlying material and also that the sedimentary beds contained more water than the flows. Such water was converted to steam and absorbed by the overflowing lava and was thus a factor in the formation of the basal amygdaloid.” (Butler & Burbank, 1929).

5.b.2. Mineralisation of the amygdales

Agate is a distinctly banded, fibrous variety of chalcedony, which is fibrous microcrystalline silica. Agate is made of layers of length-fast chalcedony, sometimes with layers of quartzine (length-slow chalcedony) fibres, and may be intergrown with moganite (a low temperature silica polymorph), α-quartz, opal-A, opal-CT and cristobalite (Michel-Lévy & Munier-Chalmas, 1892; Flörke *et al.* 1984, 1991; Heaney & Post, 1992; Cady *et al.* 1998; Hopkinson *et al.* 1999; Götze *et al.* 2020; Moxon & Palyanova, 2020). Agate generally occurs in vesicles in lavas with wall-lining banding which grows from the exterior to the interior perpendicular to the fibres. The mineralogy becomes progressively dehydrated towards the centre where quartz or amethyst may occur, or voids. The banding is due to changes in translucency as a result of changes in crystallite sizes, trace element and hydroxyl concentrations (Cady *et al.* 1998). Agate contains a significant amount of water between 0.5 and 3.0 weight% as OH in Si-OH

silanol groups (Götze et al. 2020). Agate is unusual in ageing over time. It precipitates from silicic acid (H_4SiO_4) as discrete particles (silica sols) which grow to form a gel and precipitate as amorphous silica; this changes with time to cristobalite then to fibres of chalcedony, quartzine and moganite (agate), and eventually to quartz by release of water, accompanied by an increase in crystallinity and grain size (Götze *et al.* 2020; Moxon & Palyanova, 2020). The temperature of formation of agate has been determined by various studies using oxygen and hydrogen isotopes (Fallick *et al.* 1985; Harris, 1989; Saunders, 1990), Al concentrations and fluid inclusions to be between 20 and 230°C (Götze et al., 2020), while Moxon & Palyanova (2020) concluded that the temperature of the fluid was <200°C and most likely <100°C. Agate is formed by self-organizational crystallization, as distinct from periodically changing external causes, from a fluid that is partly polymerised (Heaney, 1993) to strongly polymerised gel (Wang & Merino, 1990; Harder, 1993) or colloid (Saunders, 1990). Because of the general conditions of formation of agate, it is clear that agate deposition on Pedro Gonzalez Island took place at low temperature, after cooling of the andesite. Agate was precipitated in the open spaces of vesicles, fractures and faults to form amygdales, veins and vein breccias. The veins are commonly accompanied by intermediate argillic (probably smectite) wall rock alteration that forms at low temperature from a weakly acid hydrothermal fluid (Simmons *et al.* 2005). The presence of late-stage calcite in the small amygdales indicates that the hydrothermal fluid also contained minor amounts of CO_2 and Ca. The veins and vein breccias indicate that the lavas were subjected to brittle fracturing and faulting and imply that agate formation may be significantly younger than volcanism, in other words epigenetic, and may be related to uplift and faulting. The well-defined, focused zone of agate deposition is interpreted to represent a zone of upflow of a hydrothermal fluid which may have been related to a younger intrusion at depth (Simmons *et al.* 2005). Near-surface deposition is indicated by the low temperature of agate formation, but the environment is not constrained since agate/chalcedony deposition can take place in both submarine (Hopkinson *et al.* 1998, 1999; Franklin *et al.* 2005) and subaerial (Simmons *et al.* 2005; Hartmann *et al.* 2012) settings.

5.c. Exploitation of the agate amygdales

The 6,000-year-old shell midden archaeological site with abundant agate tools at Don Bernardo Beach occurs near the southern end of the agate zone (Fig. 3). The large size and predominance of solid agate amygdales and veins, rather than agate geodes with a void, made the agate suitable for tool manufacture, in addition to the inherent properties of hardness and conchoidal fracture (Pearson et al., 2021). The availability of raw material for tool making was undoubtedly an important factor in the location of the human settlement, and indeed it may well have been the reason for the settlement. Agate raw material could have been gathered in any of three ways: 1) by quarrying and breaking agate amygdales and veins from outcrops of andesitic lavas, although the rock is hard and this would not have been very easy and risked breakage; 2) gathering agate pebbles in the soil that have weathered out of the andesitic lavas; or 3) gathering agate pebbles from the gravel beaches. It is considered most likely that agate pebbles were collected from the soil, given that it is hard to break them from fresh andesitic lavas, and that the beach pebbles are altered to an opaque white colour from sea water interaction which may have made them unsuitable for working.

The Pedro Gonzalez agate is a geological curiosity that is likely to have limited analogues in the world. It is therefore interesting to note that the amygdaloidal basalts of the Keweenaw Series at Lake Superior, Michigan, already mentioned above (Butler & Burbank, 1929; Wilson

& Dyl, 1992), provide another example of the ancient exploitation of mineralised vesicles. Here the vesicles are locally filled with native copper, while others contain agate, and form the important mineral district of Michigan Copper Country that produced more than 5 million tonnes of copper and 500 tonnes of silver. These deposits were mined for native copper in amygdales and veins by Archaic Native Americans from 8500 to 3580 cal BP in the period known as the Old Copper Complex, one of the oldest known metalworking societies in the world (Pompeani *et al*., 2021). Copper production was from thousands of small pits, and hammering stones and copper tools have been found. The copper was used to make tools which are found widely distributed in North America.

6. Conclusions

Geological mapping, field observations and whole-rock geochemical analysis on Pedro Gonzalez Island document a submarine volcano-sedimentary sequence with distinctive lithological and geochemical characteristics that reveal the occurrence of a new "Pedro Gonzalez Formation" in the Pearl Island archipelago. This unit is composed of lavas, dykes, volcanic breccias and tuffaceous sediments that demonstrate the occurrence of active volcanic islands in the Pearl Islands in the Oligo-Miocene. Although the age of emplacement of the studied sequence have not been directly constrained, igneous rocks from Pedro Gonzalez have unique tholeiitic geochemical affinities that suggest emplacement during magmatic cessation in eastern Panama in the early Miocene (ca. 21-16 Ma). Our results suggest the existence of an uncharted Oligo-Miocene volcanic front with ancient islands in the Gulf of Panama, which might have extended across the eastern Panamanian forearc from the Canal area to the Sapo Range, but of which the exact extent and age remain to be investigated.

Agate deposits on the island are closely associated with unusually large amygdales in the submarine basaltic andesites/andesites. We suggest that these deposits formed as a result of peperitic processes from subaqueous lava-sediment interaction, whereby water released from unconsolidated tuffaceous deposits at the base of lava flows rose through the lavas, coalesced, and accumulated below the chilled lava tops. The agate deposits, hosted by submarine andesitic lavas, indicate the low temperature, shallow expression of a submarine or subaerial, epigenetic hydrothermal system. The presence of abundant agate deposits, the large amygdale size and their solid fill were important factors in the siting of the remote, insular 6,000-year-old quarry-workshop and settlement, and in fact, may have been its raison d'être.

Declaration of competing interest

The authors declare no competing interests.

Acknowledgements

Thanks are due to Richard Cooke, Senior Archaeologist, Smithsonian Tropical Research Institute, Panama City, Panama, for inviting the first author to visit the project in 2009; Juan Guillermo Martin, Professor of Archaeology, Universidad del Norte, Barranquilla, Colombia and leader of the Playa Don Bernardo rescue archaeology programme in 2015-16, for the invitation to participate in the project and for organising the site visits; Georges A. Pearson, archaeologist, Panama, who accompanied the first author on the 2015 visit; and Grupo Eleta

S.A., Panama for permitting the visits and providing transport to the island, with board and lodging, and especially for the help of their staff J. J. Amado (2009), Ignacio Solis, Irene Sathl, Angel Mendieta (logistics) and Julio Miranda (camp manager) in 2015-16; and finally to our excellent *pangero*, Angel Jiménez from Pedro de Cocal village on Pedro Gonzalez Island, who transported us around the island by boat to carry out geological mapping (2016). We thank David Muñoz and the staff at the Secretaria Nacional de Energía in Panama for providing access to unpublished drilling reports in the Gulf of Panama. Paul Hands is thanked for making the thin sections and Alastair Hodgetts for taking the photomicrographs. The comments of Léo Afraneo Hartmann and an anonymous reviewer are appreciated and helped improve the article. Field work was partly supported by grant #GEFNE137-15 of the National Geographic Society.

List of Supplementary Data

Table S1. Whole rock, major element and trace element analyses of samples from Pedro Gonzalez Island

References

Arculus, R. J. 2003. Use and abuse of the terms calcalkaline and calcalkalic. *Journal of Petrology* **44**, 929–35.

Barat, F., Mercier de Lépinay, B., Sosson, M., Müller, C., Baumgartner, P. O. & Baumgartner-Mora, C. 2014. Transition from the Farallon plate subduction to the collision between South and Central America: Geological evolution of the Panama Isthmus. *Tectonophysics* **622**, 145-67.

Barreto, C. J. S., de Lima, E. F. & Goldberg, K. 2017. Primary vesicles, vesicle-rich segregation structures and recognition of primary and secondary porosities in lava flows from the Paraná igneous province, southern Brazil. *Bulletin of Volcanology* **79**, 1-17.

Breitkreuz, C., Götze, J. & Weißmantel, A. 2021. Mineralogical and geochemical investigation of megaspherulites from Argentina, Germany, and the USA. Bulletin of Volcanology, **83**, https://doi.org/10.1007/s00445-021-01434-7.

Buchs, D. M., Baumgartner, P. O., Baumgartner-Mora, C., Flores, K. & Bandini, A. N. 2011. Upper Cretaceous to Miocene tectonostratigraphy of the Azuero area (Panama) and the discontinuous accretion and subduction erosion along the Middle American margin. *Tectonophysics* **512**, 31–46.

Buchs, D. M., Irving, D., Coombs, H., Miranda, R., Wang, J., Coronado, M., Arrocha, R., Lacerda, M., Goff, C., Almengor, E., Portugal, E., Franceschi, P., Chichaco, E. & Redwood, S. D. 2019a. Volcanic contribution to emergence of Central Panama in the Early Miocene. *Scientific Reports* **9**, 1417 (2019). https://doi.org/10.1038/s41598-018-37790-2.

Buchs, D. M., Coombs, H., Irving, D., Wang, J., Koppers, A., Miranda, R., Coronado, M., Tapia, A. & Pitchford, S. 2019b. Volcanic shutdown of the Panama Canal area following breakup of the Farallon plate. *Lithos* **334–335**, 190–204.

Butler, B. S. & Burbank, W. S., 1929. The Copper Deposits of Michigan. *United States Geological Survey Professional Paper* **144**, 238 p.

Cady, S. L., Wenk, H. R. & Sintubin, M. 1998. Microfibrous quartz varieties: characterization by quantitative X-ray texture analysis and transmission electron microscopy. *Contributions to Mineralogy and Petrology* **130**, 320-35.

Cashman, K. V. & Kauahikaua, J. P. 1997. Reevaluation of vesicle distributions in basalt lava flows. *Geology* **25**, 419-42.

Coates, A. G., Collins, L. S., Aubry, M. -P. & Berggren, W. A. 2004. The Geology of the Darien, Panama, and the late Miocene-Pliocene collision of the Panama arc with northwestern South America. *Geological Society of America Bulletin* **116**, 1327-44.

Cooke, R. G., Wake, T. A., Martínez-Polanco, M. F., Jiménez-Acosta, M., Bustamante, F., Holst, I., Lara-Kraudy, A., Martín, J. G. & Redwood, S. 2016. Exploitation of dolphins (Cetacea: Delphinidae) at a 6000 Yr old Preceramic site in the Pearl Island archipelago, Panama. *Journal of Archaeological Science: Reports* **6**, 733-56.

Derksen, S. J., Coon, H. L. & Shannon, P. J. 2003. Eastern Gulf of Panama Exploration Potential. American Association of Petroleum Geologists International Conference, Barcelona, Spain, September 21-24, 2003, 90017.

Ernst, R. E. & Jowitt, S. M., 2013. Large igneous provinces (LIP) and metallogeny. *Society of Economic Geologists Special Publication*, **17**, p. 17-51.

Fallick, A. E., Jocelyn, J., Donnelly, T., Guy, M. & Behan, C. 1985. Origin of agates in volcanic rocks from Scotland. *Nature* **313**, 672-74.

Farris, D. W., Jaramillo, C., Bayona, G., Restrepo-Moreno, S. A., Montes, C., Cardona, A., Mora, A., Speakman, R. J., Glascock, M. D. & Valencia, V. 2011. Fracturing of the Panamanian Isthmus during initial collision with South America. *Geology* **39**, 1007–10.

Farris, D. W., Cardona, A., Montes, C., Foster, D. & Jaramillo, C. 2017. Magmatic evolution of Panama Canal volcanic rocks: A record of arc processes and tectonic change. *PLos ONE* **12**, e0176010. https://doi:10.1371/journal.pone.0176010.

Flörke, O. W., Flörke, U. & Giese, U. 1984. Moganite, a new microcrystalline silica-mineral. *Neues Jahrbuch für Mineralogie, Abhandlungen* **149**, 325-36.

Flörke, O. W., Graetsch, H., Martin, B., Röller, K. & Wirth, R. 1991. Nomenclature of micro- and non-crystalline silica minerals based on structure and microstructure. *Neues Jahrbuch der Mineralogie Abhandlungen* **163**, 19-42.

Franklin, J. M., Gibson, H. L., Jonasson, I. R. & Galley, A. G. 2005. Volcanogenic massive sulfide deposits. *Economic Geology 100th Anniversary Volume*, 523-60.

Gale, A., Dalton, C. A., Langmuir, C. H., Su, Y. & Shilling, J. -G. 2013. The mean composition of ocean ridge basalts. *Geochemistry, Geophysics, Geosystems* **14**, 489–518.

Götze, J., Möckel, R. & Pan, Y., 2020. Mineralogy, geochemistry and genesis of agate – a review. *Minerals* **10**, 1037; doi:10.3390/min10111037

Harder, H. 1993. Agates - Formation as a multicomponent colloid chemical precipitation at low temperatures. *Neues Jahrbuch für Mineralogie* **1**, 31–48.

Harris, C. 1989. Oxygen-isotope zonation of agates from Karoo volcanics of the Skeleton Coast, Namibia. *American Mineralogist* **74**, 476-81.

Hartmann, L. A. & Duarte, S. K., 2020. Novo Hamburgo Complex formed by hydrothermal, explosive injection of Botucatu erg sand into extensive tracts of Paraná Volcanic Province. *Journal of Sedimentary Environments* **5**, 187-198

Hartmann, L. A., da Cunha Duarte, L., Massonne, H. -J., Michelin, C., Rosenstengel, L. M., Bergmann, M., Theye, T., Pertille, J., Arena, K. R., Duarte, S. K., Pinto, V. M., Barboza, E. G., Rosa, M. L. C. C. & Wildner, W. 2012. Sequential opening and filling of cavities forming vesicles, amygdales and giant amethyst geodes in lavas from the southern Paraná volcanic province, Brazil and Uruguay. *International Geology Review* **54**, 1-14.

Heaney, P. J. 1993. A proposed mechanism for the growth of chalcedony. *Contributions to Mineralogy and Petrology* **115**, 66–74.

Heaney, P. J. & Post, J. E. 1992. The widespread distribution of a novel silica polymorph in microcrystalline quartz varieties. *Science* **255**, 441-3.

Hopkinson, L., Roberts, S., Herrington, R. & Wilkinson, J. 1998. Self-organization of submarine hydrothermal siliceous deposits: Evidence from the TAG hydrothermal mound, 26°N Mid-Atlantic Ridge. *Geology* **26**, 347-50.

Hopkinson, L., Roberts, S., Herrington, R. & Wilkinson, J. 1999. The nature of crystalline silica from the TAG submarine hydrothermal mound, 26°N Mid-Atlantic Ridge. *Contributions to Mineralogy and Petrology* **137**, 342-50.

Kirby, M. X., Jones, D. S. & MacFadden, B. J. 2008. Lower Miocene Stratigraphy along the Panama Canal and Its Bearing on the Central American Peninsula. *Plos ONE* **3**, e2791. https://doi:org/10.1371/journal.pone.

Kolarsky, R. A., Mann, P., Monechi, S., Meyerhoff, H. D. & Pessagno, E. A. 1995. Stratigraphic development of southwestern Panama as determined from integration of marine seismic data and onshore geology. In *Geologic and tectonic development of the Caribbean plate boundary in southern Central America* (ed P. Mann), pp. 159-200. Geological Society of America, Special Paper no. 295.

Krawinkel, H., Wozazek, S., Krawinkel, J. & Hellmann, W. 1999. Heavy-mineral analysis and clinopyroxene geochemistry applied to provenance analysis of lithic sandstones from the Azuero-Sona Complex (NW Panama). *Sedimentary Geology* **124**, 149–68.

Lissinna, B. 2005. A profile through the Central American landbridge in western Panama: 115 Ma interplay between the Galápagos hotspot and the Central American subduction zone. PhD thesis, Christian-Albrechts-Univesität, Kiel, Germany. Published thesis.

MacFadden, B. J., Bloch, J. I., Evans, H., Foster, D. A., Morgan, G. S., Rincon, A. & Wood, A. R. 2014. Temporal calibration and biochronology of the Centenario fauna, Early Miocene of Panama. *The Journal of Geology* **122**, 113–35.

Mann, P. & Kolarsky, R. A. 1995. East Panama deformed belt: Structure, age, and neotectonic significance. In *Geologic and tectonic development of the Caribbean plate boundary in southern Central America* (ed P. Mann), pp. 111-130. Geological Society of America, Special Paper no. 295.

Martín, J. G., Cooke, R. G., Bustamante, F., Holst, I., Lara, A. & Redwood, S. 2016. Ocupaciones prehispánicas en Isla Pedro González, Archipiélago de las Perlas, Panamá. Aproximación a una cronología con comentarios sobre las conexiones externas. *Latin American Antiquity* **27**, 378-96.

Michel-Lévy, A. & Munier-Chalmas, C. P. E. 1892. Mémoire sur diverses formes affectées par le réseau élémentaire du quartz. *Bulletin de la Société Française de Minéralogie* **15**, 159-90.

Montes, C., Bayona, G., Cardona, A., Buchs, D. M., Silva, C. A., Morón, S., Hoyos, N., Ramírez, D. A., Jaramillo, C. A. & Valencia, V. 2012a. Arc-continent collision and orocline formation: Closing of the Central American seaway. *Journal of Geophysical Research* **117**, B04105. https://doi.org/10.1029/2011JB008959.

Montes, C., Cardona, A., McFadden, R., Morón, S. E., Silva, C. A., Restrepo-Moreno, S., Ramírez, D. A., Hoyos, N., Wilson, J., Farris, D., Bayona, G. A., Jaramillo, C. A., Valencia, V., Bryan, J. & Flores, J. A. 2012b. Evidence for middle Eocene and younger land emergence in central Panama: Implications for Isthmus closure. *Geological Society of America Bulletin* **124**, 780-99.

Montes, C., Cardona, A., Jaramillo, C., Pardo, A., Silva, J. C., Valencia, V., Ayala, C., Pérez-Angel, L. C., Rodriguez-Parra, L. A., Ramirez, V. & Niño, H. 2015. Middle Miocene closure of the Central American Seaway. *Science* **348**, 226–9.

Moxon, T. & Palyanova, G. 2020. Agate genesis: A continuing enigma. *Minerals* **10**, 953; doi:10.3390/min10110953

Nicholson, S. W., Cannon, W. F. & Schulz, K. J., 1992. Metallogeny of the Midcontinent rift system of North America. *Precambrian Research* **58**, p. 355–86.

Pearce, J. A. 2008. Geochemical fingerprinting of oceanic basalts with applications to ophiolite classification and the search for Archean oceanic crust. *Lithos* **100**, 14–48.

Pearson, G. A., Martín, J. G., Castro, S. A., Acosta, M. A. & Cooke, R. G. 2021. The mid Holocene occupation of the Pearl Islands: A case of unusual insular adaptations on the Pacific coast of Panama. *Quaternary International* **578**, 155-69.

Pompeani, D. P., Steinman, B. A., Abbott, M. B., Pompeani, K. M., Reardon, W., DePasqual, S. & Mueller, R. H. 2021. On the timing of the Old Copper Complex in North America: A comparison of radiocarbon dates from different archaeological contexts. *Radiocarbon* **63**, p. 513-531, https://:doi.org/ 10.1017/RDC.2021.7.

Quirós Ponce, J. L. 1975. Las exploraciones petroleras en Panamá. In *Apuntes sobre recursos minerales en Panamá* (J. L. Quirós Ponce), pp. 29-35. Dirección General de Recursos Minerales, Panama, Panama.

Redwood, S. D. 2020. Late Pleistocene to Holocene sea level rise in the Gulf of Panama, Panama and its influence on early human migration through the Isthmus. *Caribbean Journal of Earth Science* **51**, 15-31.

Rooney, T., Franceschi, P. & Hall, C. 2011. Water-saturated magmas in the Panama Canal region: a precursor to adakite-like magma generation? *Contributions to Mineralogy and Petrology* **161**, 373–88.

Retallack, G. J. & Kirby, M. X. 2007. Middle Miocene global change and paleogeography of Panama. *PALAIOS* **22**, 667-79.

Saunders, J. A. 1990. Oxygen-isotope zonation of agates from Karoo volcanics of the Skeleton Coast, Namibia: Discussion. *American Mineralogist* **75**, 1205-6.

Schmidt, M. W. & Jagoutz, O. 2017. The global systematics of primitive arc melts. *Geochemistry, Geophysics, Geosystems* **18**, 2817–54.

Self S., Thordarson, T., Keszthelyi, L., Walker, G. P. L., Hon, K., Murphy, M. T., Long, P. & Finnemore, S. 1996. A new model for the emplacement of Columbia River Basalts as large inflated pahoehoe lava flow fields. *Geophysical Research Letters* **23**, 2689-92.

Self, S., Thordarson, T. & Keszthelyi, L. 1997. Emplacement of continental flood basalt lava flows. In *Large Igneous Provinces: Continental, Oceanic, and Planetary Flood Volcanism*. (eds J. J. Mahoney and M. Coffin), pp. 381-410. American Geophysical Union, Geophysical Monograph no. 100.

Self, S., Keszthelyi, L. & Thordarson, T. 1998. The importance of pahoehoe. *Annual Review of Earth and Planetary Sciences* **26**, 81-100.

Shea, T., Houghton, B. F., Gurioli, L., Cashman, K., Hammer, J. E. & Hobden, B. J. 2010. Textural studies of vesicles in volcanic rocks: an integrated methodology. *Journal of Volcanology of Geothermal Research* **190**, 271–289.

Shipboard Scientific Party, 2000. Site 1139. In *Proceedings of the Ocean Drilling Program, Initial Reports, vol. 183* (M. F. Coffin, F. A. Frey, P. J. Wallace et al.), pp. 1-213. College Station, Texas.

Simmons, S., White, N. C. & John, D. A. 2005. Geological characteristics of epithermal precious and base metal deposits. *Economic Geology 100th Anniversary Volume*, 485-522.

Skilling, I. P., White, J. D. L. & McPhie, J. 2002. Peperite: a review of magma-sediment mingling. *Journal of Volcanology and Geothermal Research* **114**, 1-17.

Thordarson, T. 2000. Physical volcanology of lava flows on Surtsey, Iceland: A preliminary report. *Surtsey Research* **11**, 109-26.

Wang, Y. & Merino, E. 1990. Self organization origin of agates: Banding, fibre twisting, composition and dynamic crystallization model. *Geochimica et Cosmochimica Acta* **54**, 1627–38.

Whattam, S. A., Montes, C., McFadden, R. R., Cardona, A., Ramirez, D. & Valencia, V. 2012. Age and origin of earliest adakitic-like magmatism in Panama: implications for the tectonic evolution of the Panamanian magmatic arc system. *Lithos* **142-143**, 226-44.

Wilson, M. L. & Dyl, S. J., II 1992. The Michigan Copper Country. *The Mineralogical Record*, **23**, p. 1-72.

.

Figures

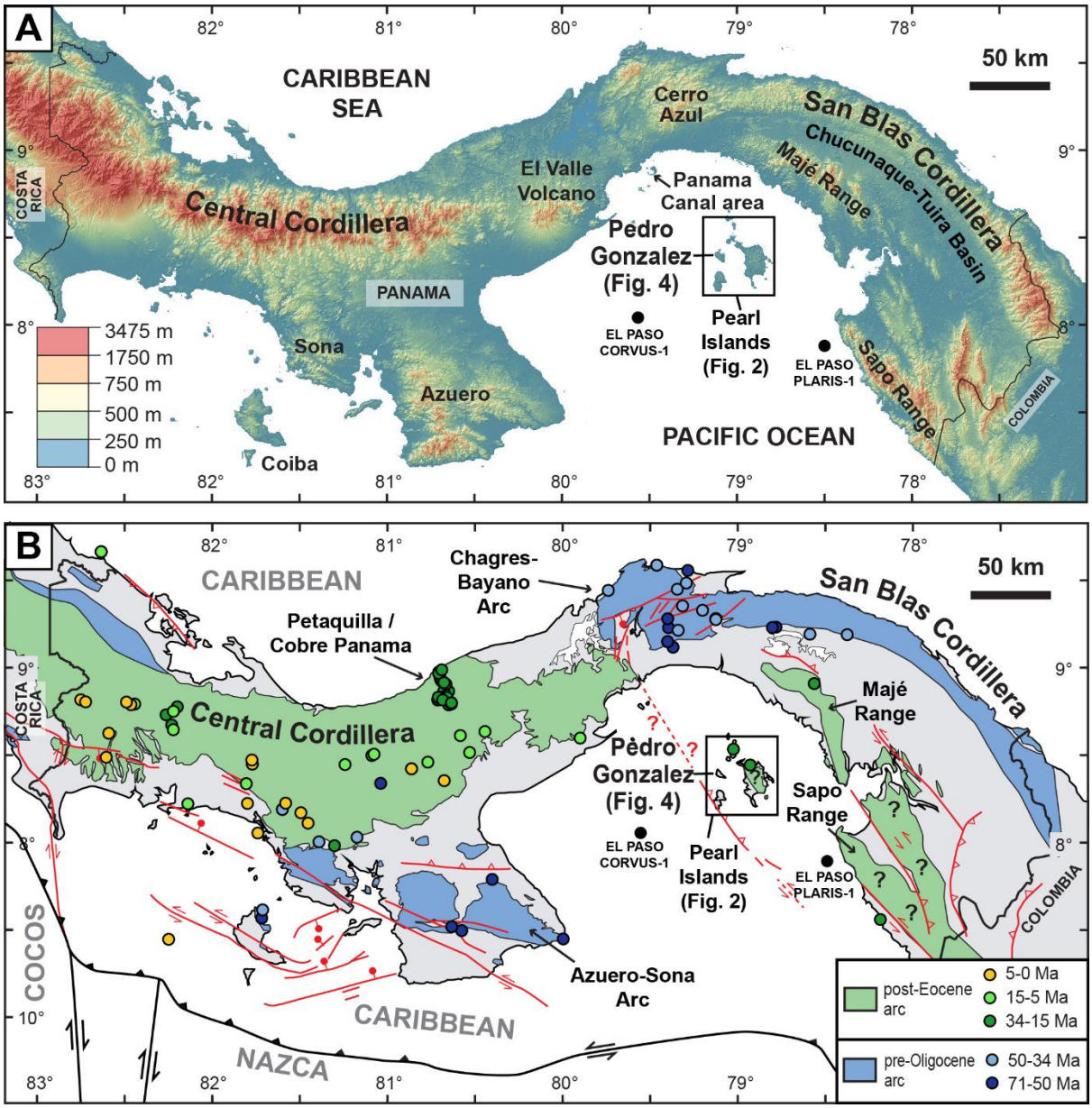

Figure 1. Regional geological setting of the Pearl Islands and Pedro Gonzalez Island showing the location of the El Paso Corvus-1 and El Paso Plaris-1 drill holes (modified from Buchs *et al.* 2019b).

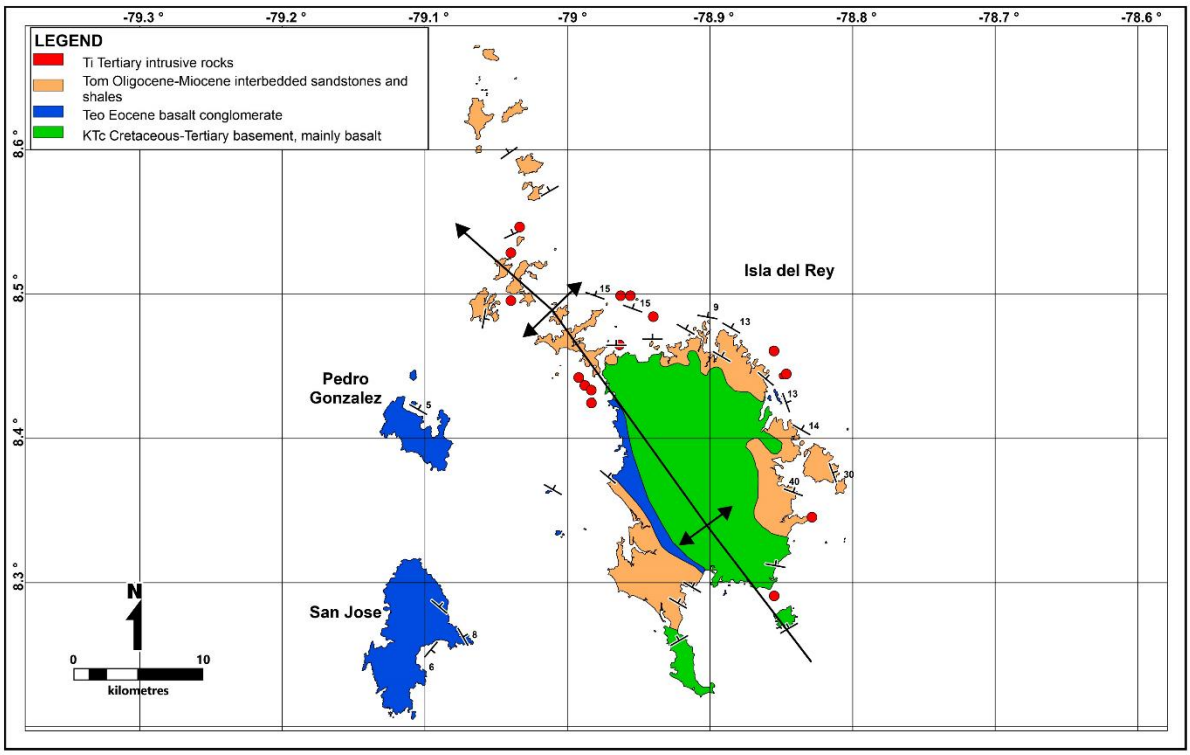

Figure 2. Geologic compilation map of the Pearl Islands Archipelago (adapted from Mann & Kolarsky, 1995).

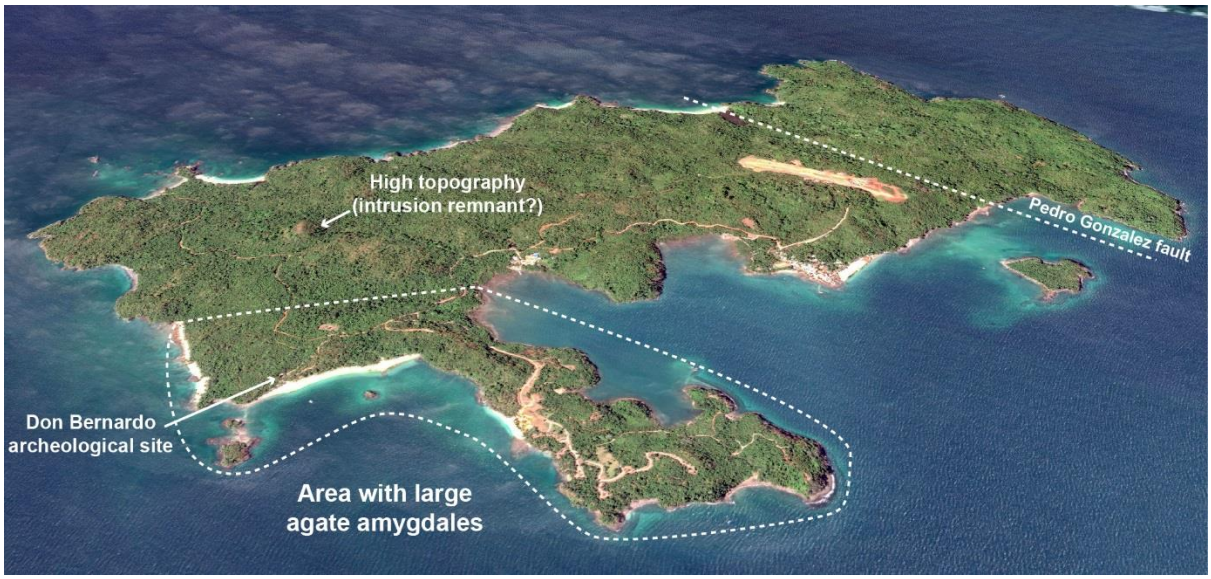

Figure 3. Satellite view towards the SW of Pedro Gonzalez Island, showing the area containing large agate amygdales (image captured in 2013, source: Google Earth).

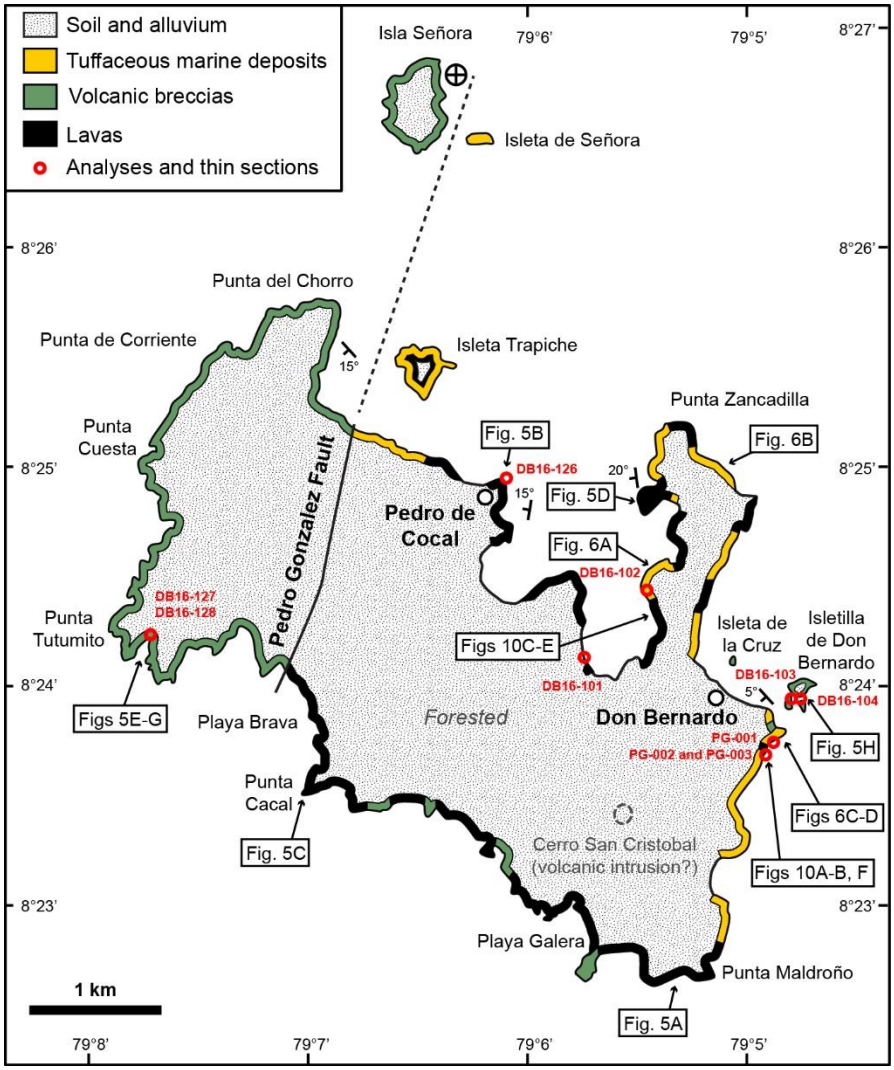

Figure 4. Geological map of Pedro Gonzalez Island. Ubiquitous faulting impedes interpretation of the inland geology. The location of the rock photographs (Figs. 5, 6 and 10) are shown, and the samples that were analysed and thin sectioned with photomicrographs (Figs. 7 and 11).

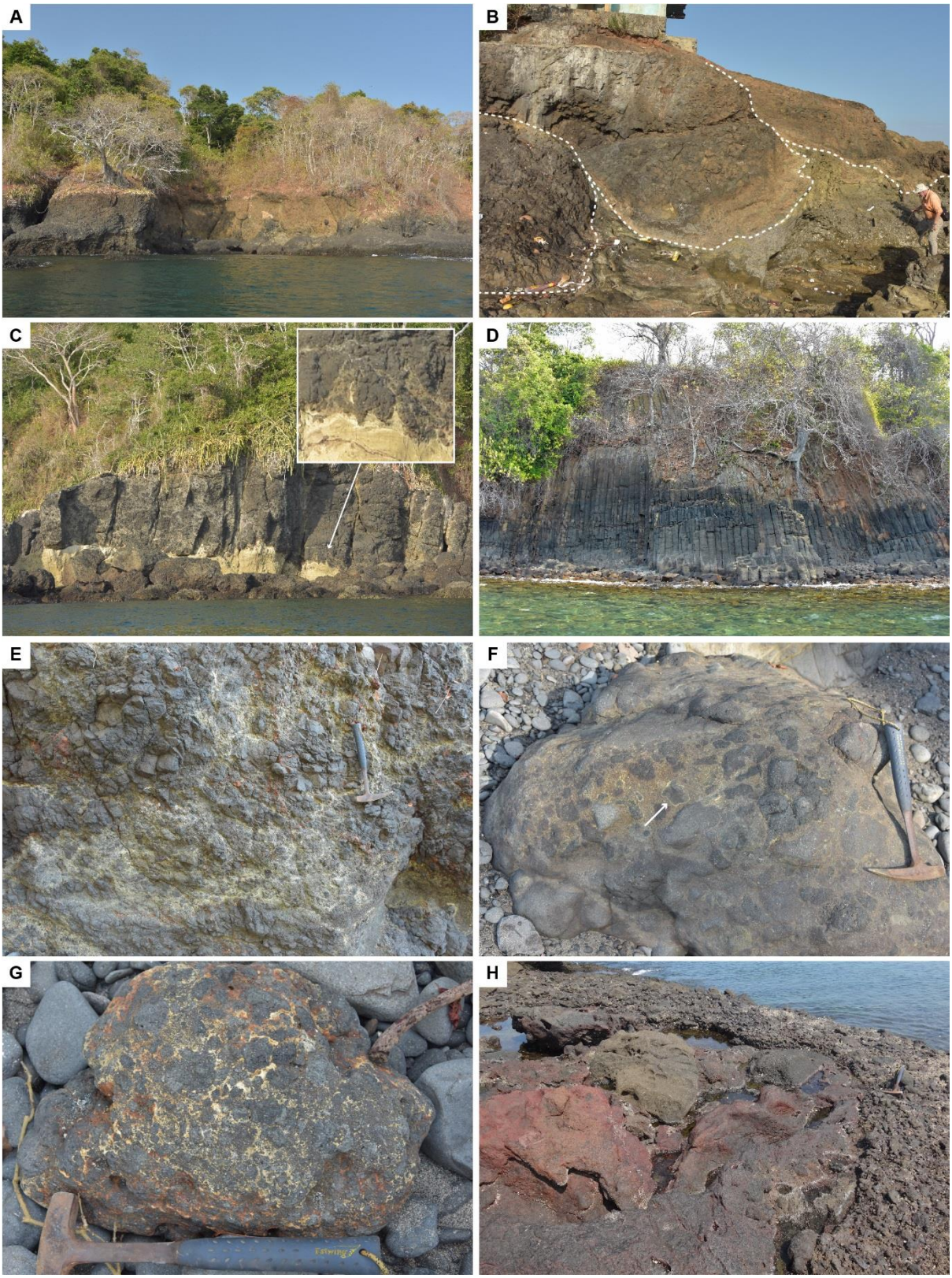

Figure 5. Examples of andesitic lavas and primary andesitic breccias exposed along the coast of Pedro Gonzalez Island (location of the pictures is shown in Fig. 4). A) Lavas interbedded with tuffaceous marine deposits (exposure height is approximately 7 m). Lava on the left has columnar joints curving close to the margin of the flow, whereas the lava on the right is massive with breccias at its top. B) Lava lobes impinging upon tuffaceous deposits. C) Massive

to brecciated lava with evidence of soft deformation of tuffaceous deposits at its base. Brecciation occurs close to the margin of the flow on both sides of the picture. D) Thick lava with large near-vertical columnar jointing (exposure height is approximately 8 m). E) Monomictic breccia with elongated lava fragments. This lithology is chiefly layered at the metre scale and forms most of the volcaniclastic deposits west of the Pedro Gonzalez fault. F) Block of monomictic breccia with chilled amoeboid clasts (arrow). G) Block of monomictic breccia with amoeboid clasts and a palagonized glassy or tuffaceous matrix. H) Lobate lava intruding andesite breccias.

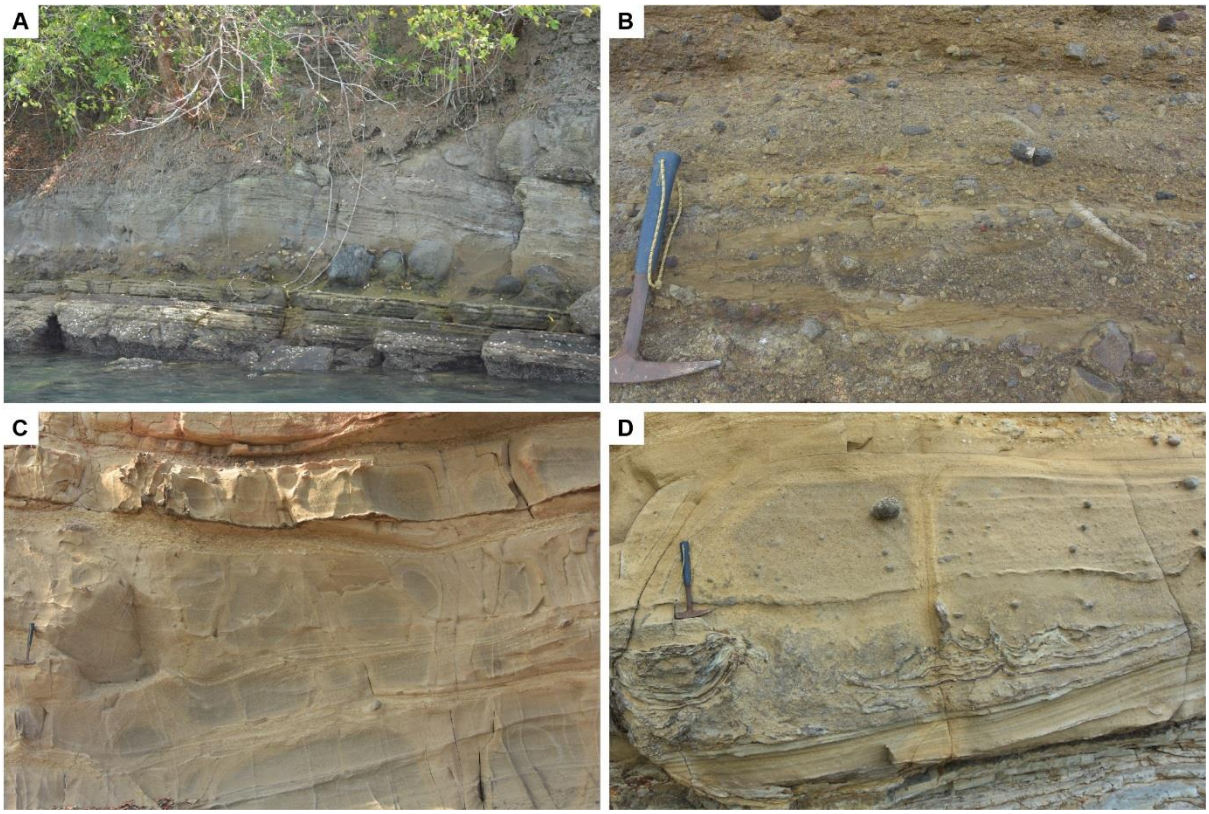

Figure 6. Examples of tuffaceous marine deposits exposed along the coast of Pedro Gonzalez Island (location of the pictures is shown in Fig. 4). A) Tuffaceous deposits with cross- to parallel-layered, fine to coarse tuffs and tuffaceous (matrix-supported) debris-flow deposits containing andesite granules to boulders. Some of the larger clasts in the debris flow deposits are well-rounded. B) Lenses of polymictic andesitic breccia interbedded with tuffaceous deposits. Note burrows that occur as cm-wide tubes crosscutting the bedding. C) Cross-bedded marine tuffaceous deposits with whiter pumiceous beds. D) Fluid escape structures in tuffaceous deposits.

Figure 7

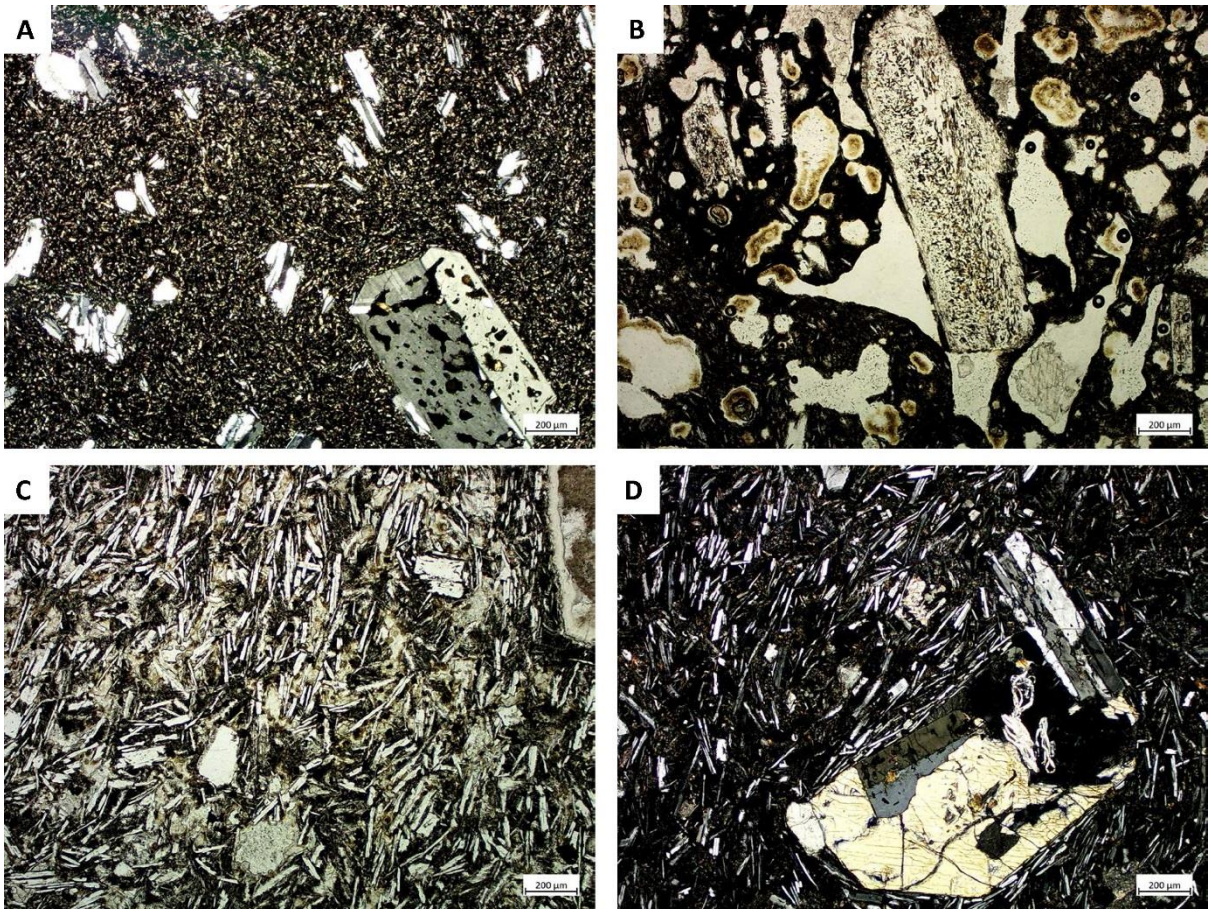

Figure 7. Photomicrographs of volcanic rock textures (sample locations are shown in Fig. 4). A) Fine grained, columnar jointed basalt with plagioclase phenocrysts and microcrystals of plagioclase in a very fine grained matrix (DB16-101, xp). B) Clast in breccia of vesicular basalt with plagioclase phenocrysts. Small vesicles are lined with an acicular brown mineral, possibly a zeolite. (DB16-104, ppl). C) Amygdaloidal lava with plagioclase microphenocrysts in a matrix with abundant plagioclase laths with a trachytic texture (PG-002, ppl). D) Amygdaloidal lava with a large phenocryst of plagioclase and clinopyroxene in a matrix with abundant plagioclase laths with a trachytic texture (PG-002, xp). Abbreviations: ppl - plane polarised light; xp - crossed polars.

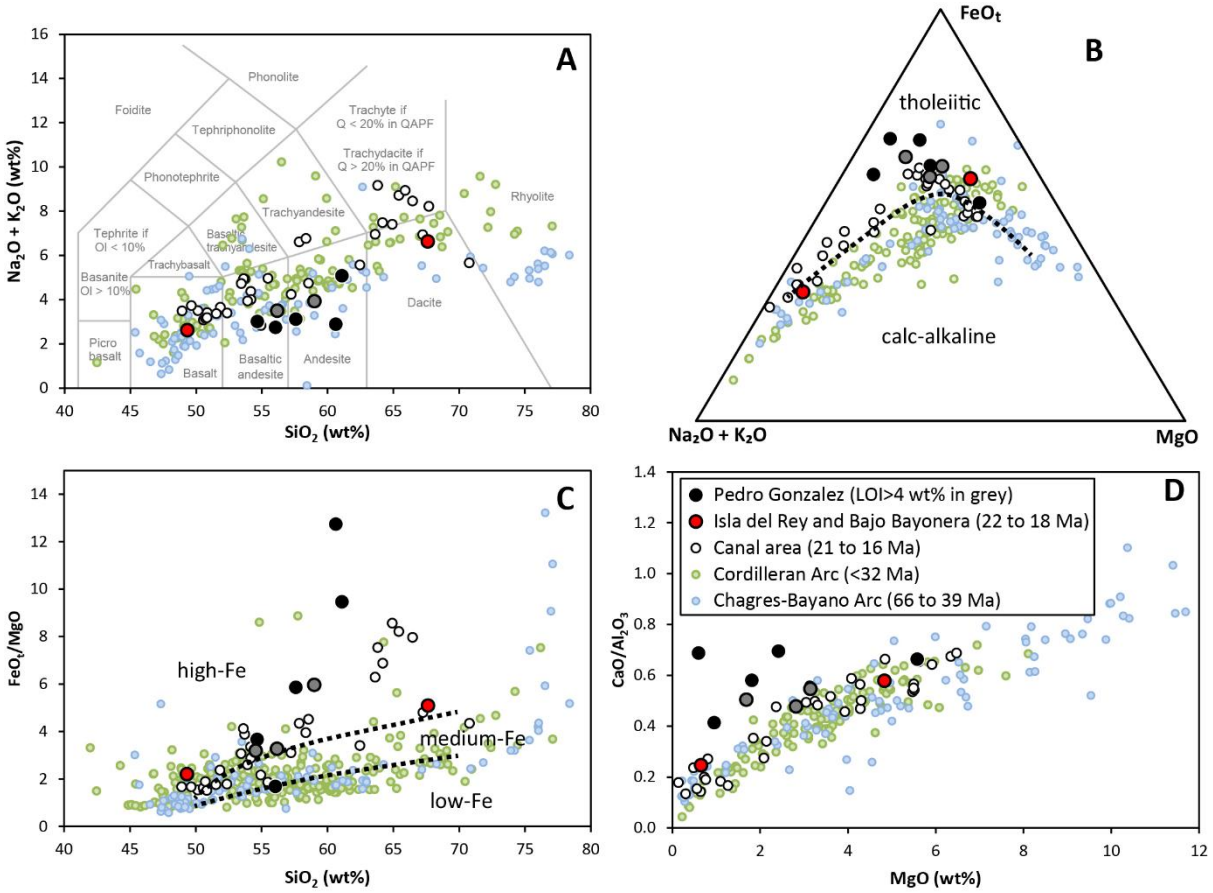

Figure 8. Major element diagrams showing igneous rocks from Pedro Gonzalez Island (lavas, clast and dykes, location shown in Fig. 4) and regional volcanic arc units. Sources and handling of the data are detailed in the Methods. SiO_2 vs FeO*/MgO diagram is after Arculus (2003).

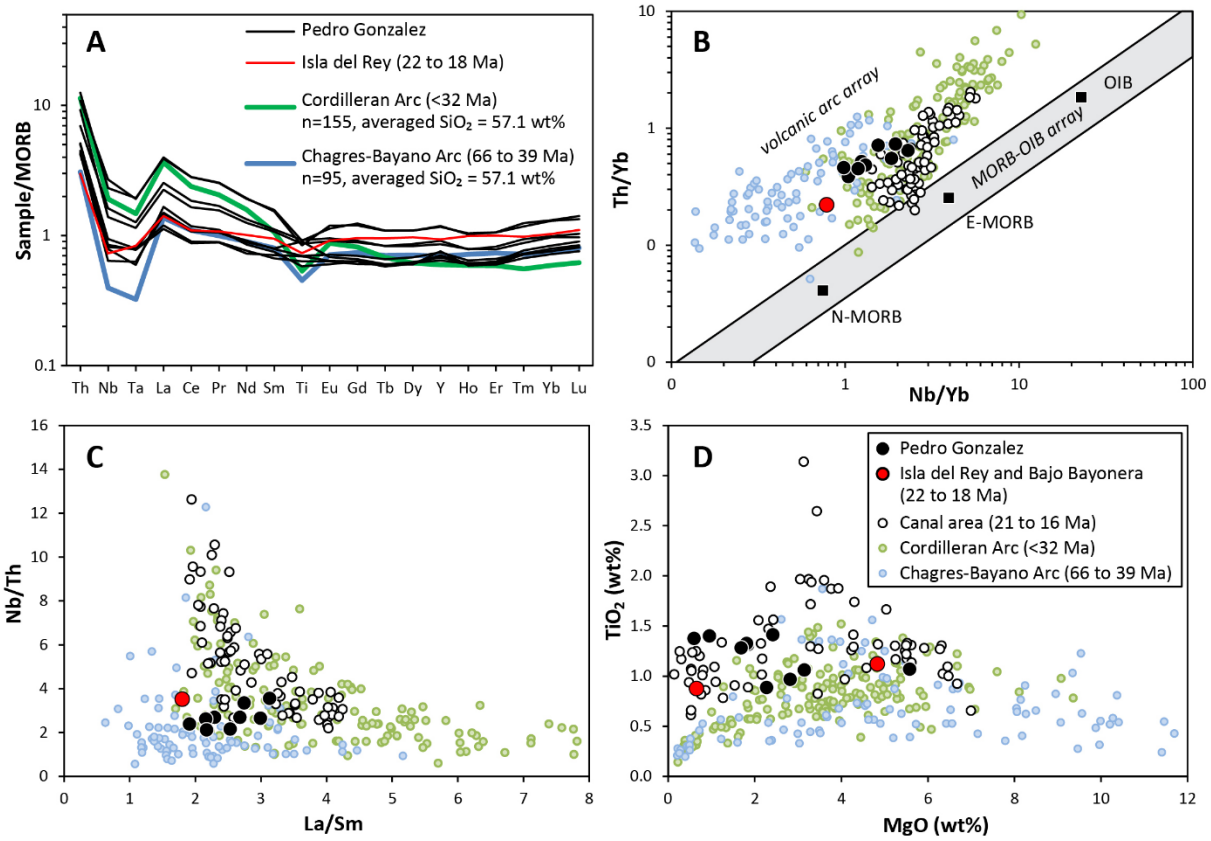

Figure 9. Trace element diagrams showing igneous rocks from Pedro Gonzalez Island (lavas, clast and dykes, location shown in Fig. 4) and regional volcanic arc units. Sources and handling of the data are detailed in the Methods. MORB normalisation values in (A) are from Gale et al. (2013). Nb/Yb vs Th/Yb diagram is after Pearce (2008).

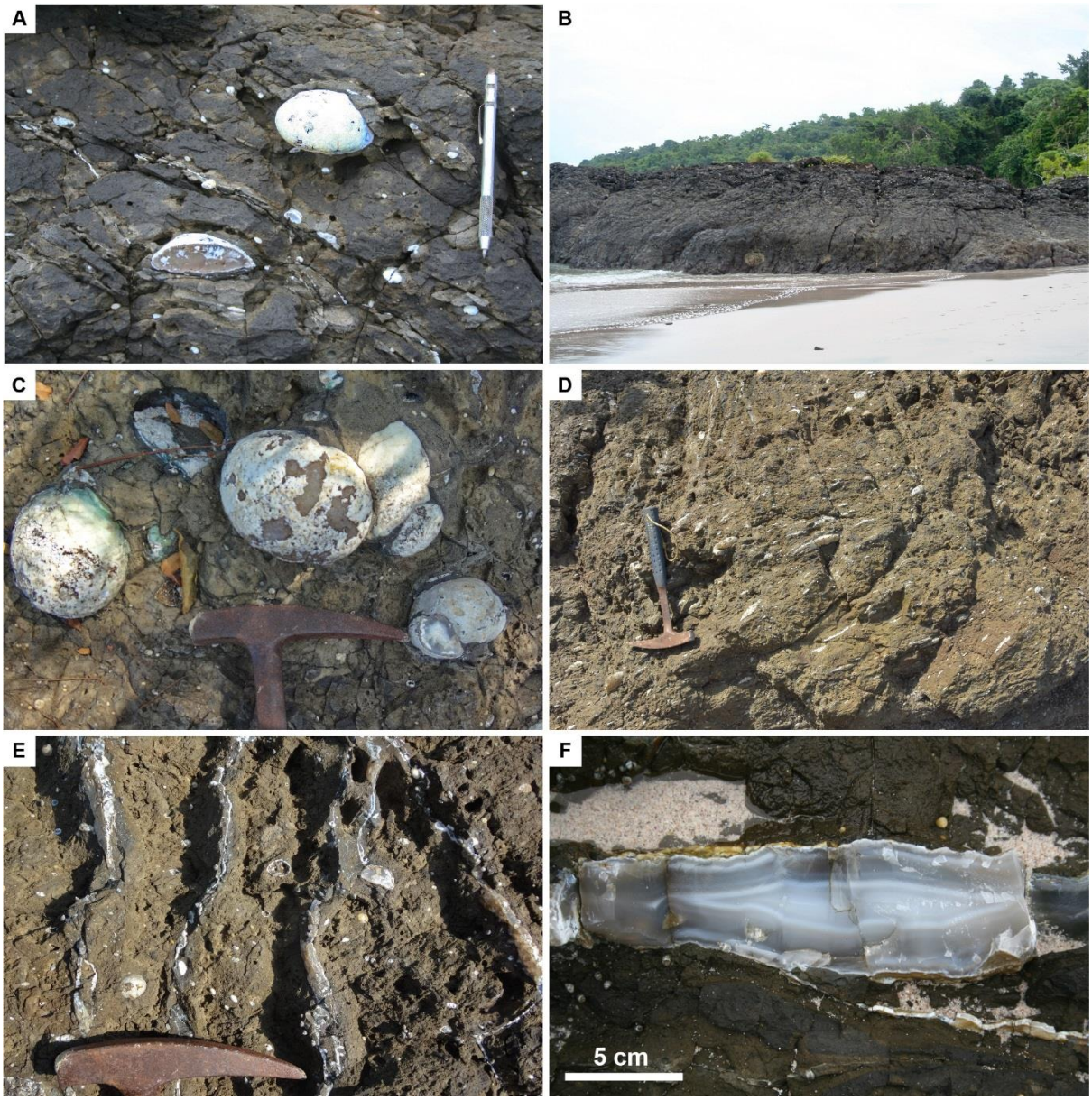

Figure 10. Examples of large agate amygdales and veins (location of the pictures is shown in Fig. 4). A) Spherical to oblong, bimodal small and large amygdales in a massive tabular lava interbedded with marine tuffaceous deposits (lava shown in [B]). B) Massive tabular lava with concentration of larger amygdales at the top (approximate height of the outcrop is 4 m). C) Coalescence of large amygdales in a lobate lava. D) Elongated amygdales in a lobate lava with the maximal length of the agates parallel to the flow. E) Irregular agate veins in a lobate lava with large amygdales. F) Thicker agate veins in massive tabular lava (B) showing concentric banding.

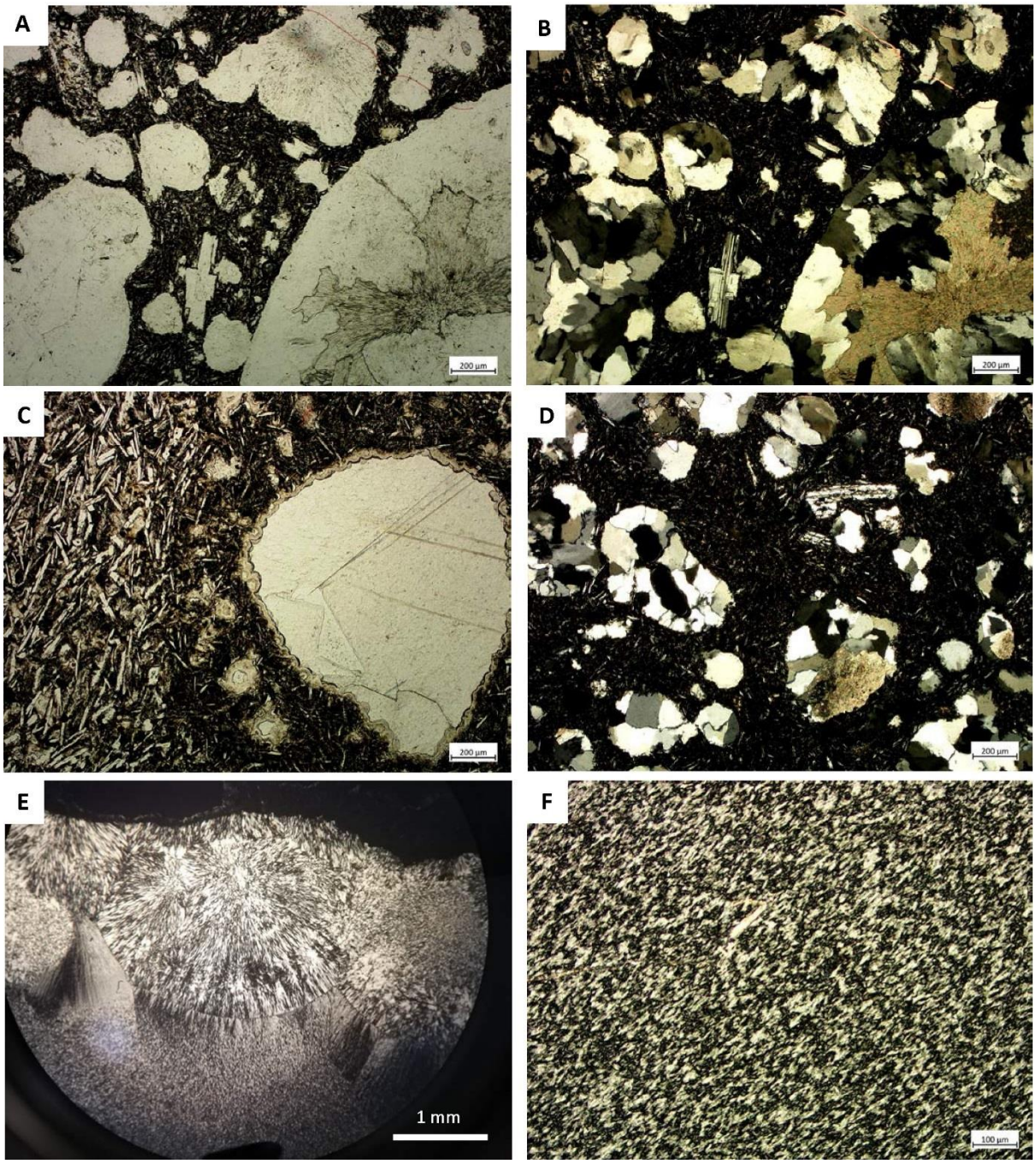

Figure 11. Amygdale photomicrographs (sample locations are shown in Fig. 4). A, B) Vesicular basalt clast in breccia with small amygdales with infill of quartz with calcite in the centre (DB16-104, ppl (A), xp (B)). C) Amygdaloidal lava with small amygdale with a wall-contact layer of low birefringence mineral (quartz or zeolite?) that is coated by an unidentified brown botryoidal mineral and filled with coarse calcite (PG-002, ppl). D) Small amygdales with infill of quartz and minor calcite in vesicular basalt clast in breccia (DB16-104, xp). E) Chalcedony with fibrous radial texture in spherules on the edge of a giant agate amygdale, with microfibrous textured chalcedony in the middle (PG-003, xp). F) Chalcedony with microfibrous texture in a giant agate amygdale (PG-003, xp). Abbreviations: ppl - plane polarised light; xp - crossed polars.